ELSEVIER

Advances in Water Resources 23 (1999) 217–228

Advances in Water Resources

Analytical approximation to characterize the performance of in situ aquifer bioremediation

H. Keijzer [a,*], M.I.J. van Dijke [b], S.E.A.T.M. van der Zee [a]

[a] *Department of Environmental Sciences, Wageningen Agricultural University, P.O. Box 8005, 6700 EC Wageningen, The Netherlands*
[b] *Department of Petroleum Engineering, Heriot-Watt University, Edinburgh EH14 4AS, UK*

Received 13 November 1998; accepted 23 March 1999

Abstract

The performance of in situ bioremediation to remove organic contaminants from contaminated aquifers depends on the physical and biochemical parameters. We characterize the performance by the contaminant removal rate and the region where biodegradation occurs, the biologically active zone (BAZ). The numerical fronts obtained by one-dimensional in situ bioremediation modeling reveal a traveling wave behavior: fronts of microbial mass, organic contaminant and electron acceptor move with a constant velocity and constant front shape through the domain. Hence, only one front shape and a linear relation between the front position and time is found for each of the three compounds. We derive analytical approximations for the traveling wave front shape and front position that agree perfectly with the traveling wave behavior resulting from the bioremediation model. Using these analytical approximations, we determine the contaminant removal rate and the BAZ. Furthermore, we assess the influence of the physical and biochemical parameters on the performance of the in situ bioremediation technique.

Keywords: Biodegradation; Transport; Traveling wave; Analytical approximation

Notation

$c(C)$	(Dimensionless) concentration electron acceptor (kg m^{-3})
c_0	Feed concentration electron acceptor (kg m^{-3})
C_{cons}	Amount of electron acceptor consumed (kg)
C_{inj}	Amount of injected electron acceptor (kg)
C_{pres}	Amount of electron acceptor present in domain (kg)
C_r	Critical electron acceptor concentration (kg m^{-3})
D	Dispersion coefficient (m^2 day^{-1})
$g(G)$	(Dimensionless) concentration organic contaminant (kg m^{-3})
g_0	Initial concentration organic contaminant (kg m^{-3})
G_{C}	Consumed contaminant concentration (kg m^{-3})
$k_c(K_C)$	(Dimensionless) electron acceptor half saturation constant (kg m^{-3})
$k_g(K_G)$	(Dimensionless) organic contaminant half saturation constant (kg m^{-3})
L	Length of initial contaminated aquifer (m)
L_k	Damkohler number
$m(M)$	(Dimensionless) concentration microbial mass (kg m^{-3})
m_0	Initial concentration microbial mass (kg m^{-3})
$m_{\max}$	Maximal concentration microbial mass (kg m^{-3})
$m_c(M_C)$	(Dimensionless) stoichiometric coefficient (kg kg^{-1})
$m_g(M_G)$	(Dimensionless) stoichiometric coefficient (kg kg^{-1})
M_{RG}	Dimensionless cumulative contaminant removal
M_1	First moment (m)
M_2^c	Second central moment (m^2)
n	Porosity
P_e	Peclet number
r_g, (R_G)	(Dimensionless) contaminant removal rate (kg day^{-1})
$t(T)$	(Dimensionless) time (day)
v	Flow velocity (m day^{-1})

* Corresponding author. Tel.: +31 7 483641; fax: +31 7 483766; e-mail: henriette.keijzer@bodhyg.benp.wau.nl

0309-1708/99/$ - see front matter
PII: S0309-1708(99)00012-3

$x(X)$	(Dimensionless) length (m)
α	Dimensionless traveling wave velocity
α_l	Dispersivity (m)
ϵ	Small number (kg m^{-3})
η	Moving coordinate
μ_m	Maximum specific growth rate (day^{-1})

1. Introduction

One of the approaches to remove organic contaminants from the aquifer is in situ bioremediation. This approach is applicable if micro-organisms are present in the subsoil that can degrade organic contaminants with the help of an electron acceptor. If the micro-organisms aerobically degrade the organic contaminant, oxygen may act as an electron acceptor. At smaller redoxpotentials, other compounds (e.g. nitrate, Fe(III), or sulfate) may serve as the electron acceptor [20]. Provided that an electron acceptor is suffciently available, the micro-organism population may grow during the consumption of organic contaminant. Hence, injection of a dissolved electron acceptor in a reduced environment may enhance the biodegradation rate.

In this study, we use two factors to characterize the performance of bioremediation: the overall contaminant removal rate and the region where biodegradation occurs, the biologically active zone (BAZ) of the aquifer [15,16]. The contaminant removal rate describes how fast the contaminant is removed from an aquifer. It is based on the averaged front position. The BAZ, which we based on the front shape of the electron acceptor, describes the transition of contaminant concentration from the remediated part to the contaminated part of the aquifer. If a small BAZ develops, there is a clear distinction between the part of the aquifer that is still contaminated and the part that has already been remediated. If the BAZ is large, the electron acceptor may already reach an extraction well while there is still a large amount of contaminant available. This indicates a less effcient use of injected electron acceptor.

The contaminant removal rate and the BAZ are affected by the physical and biochemical parameters of the soil. Insight into these effects is important for determining the performance of the in situ bioremediation technique. Numerical models or analytical solutions can be used to determine the effects of the different parameters. Several researchers have developed numerical models that include transport and biodegradation. These models are used to simulate laboratory [5,6,25] or field [3,13,19] experiments or to gain better understanding of the underlying processes [11,12,15,16]. The models differ with respect to assumptions made concerning, e.g. the number of involved compounds, the biodegradation kinetics and the mobility of the compounds. A detailed overview of various numerical bioremediation models is given by Baveye and Valocchi [1] and Sturman et al. [21].

Moreover, Oya and Valocchi [15,16] and Xin and Zhang [24] have studied in situ bioremediation analytically. Oya and Valocchi [15,16] present an analytical expression for the long-term degradation rate of the organic pollutant, derived from a simplified conceptual bioremediation model. Xin and Zhang [24] derive (semi-) analytical solutions for the contaminant and electron acceptor front shapes, using a two component model. This two component model results from the model used by Oya and Valocchi by neglecting dispersion and setting the biomass kinetics to equilibrium. In our study, we derive analytical approximations for the contaminant and electron acceptor front shapes for another simplified model. We also use the model of Oya and Valocchi and consider an immobile contaminant and a specific growth rate which is significantly larger than the decay rate. Our special interest goes to the influence of the physical and biochemical properties of the soil on the performance of the in situ remediation. We use the analytical approximations of the front shapes to show in more detail how various model parameters affect the contaminant removal rate and the BAZ.

2. Mathematical formulation

We consider the same one-dimensional bioremediation model as Keijzer et al. [11]. A saturated and homogeneous aquifer with steady-state flow is assumed. The model includes three mass balance equations, one for the electron acceptor c, one for the organic contaminant g and one for the microbial mass m. Several simplifying assumptions are made. We consider a mobile and non-adsorbing electron acceptor, e.g. oxygen or nitrate. The electron acceptor is injected to enhance biodegradation [3,15,16,24]. Although the contaminant is often considered mobile [3,15,16,24], we assume an immobile contaminant. This assumption reflects the situation where a contaminant is present at residual saturation, furthermore, the contaminant has a low solubility. We consider the effect of this assumption on the contaminant removal rate in the discussion and compare our findings with Oya and Valocchi [15] who have considered a mobile and linear-adsorbing contaminant. Moreover, we consider an immobile microbial mass that forms biofilms around the soil particles [5,9,13]. The micro-organisms are assumed to utilize the residual contaminant for their metabolism. The microbial growth is modeled by Monod kinetics, [14–16,24] the micro-organisms grow until the contaminant or electron acceptor is completely consumed. Furthermore, we neglect the decay of micro-organisms, assuming that the specific growth rate is significantly larger than the

decay rate. Because of this assumption, we might obtain a large maximum microbial mass when the initial contaminant concentration is large. These assumptions lead to the following mass balance equations for the three components:

$$\frac{\partial c}{\partial t} = D\frac{\partial^2 c}{\partial x^2} - v\frac{\partial c}{\partial x} - m_c\frac{\partial m}{\partial t}, \tag{1}$$

$$\frac{\partial m}{\partial t} = \mu_{\mathrm{m}}\left(\frac{c}{k_c + c}\right)\left(\frac{g}{k_g + g}\right)m, \tag{2}$$

$$\frac{\partial g}{\partial t} = -m_g\frac{\partial m}{\partial t}, \tag{3}$$

where D denotes the dispersion coefficient and v the effective velocity. The parameters in Eq. (2) are the maximum specific growth rate, μ_{m}, and the dissolved electron acceptor and organic contaminant half saturation constants, k_c and k_g. The stoichiometric parameters m_c and m_g in these equations describe, respectively, the ratios of consumed electron acceptor and organic contaminant to newly formed micro-organism.

Initially, at $t = 0$, we consider a constant contaminant concentration, g_0, and a constant, small microbial mass, m_0, in the domain. We assume the electron acceptor concentration to be the limiting factor for biodegradation which is initially equal to zero. At the inlet of the domain a prescribed mass flux of the electron acceptor is imposed and at the outlet ($x = L$) we assume a purely advective mass flux of the electron acceptor. Hence, the initial and boundary conditions are

$$-D\frac{\partial c}{\partial x} + vc = vc_0 \quad \text{for } t > 0 \text{ at } x = 0, \tag{4}$$

$$\frac{\partial c}{\partial x} = 0 \quad \text{for } t > 0 \text{ at } x = L, \tag{5}$$

$$c = 0,\ m = m_0,\ g = g_0 \quad \text{for } x \geqslant 0 \text{ at } t = 0. \tag{6}$$

We introduce dimensionless quantities [6,10,11]:

$$\begin{aligned} &X = \frac{x}{L}, \quad T = \frac{vt}{L}, \\ &C = \frac{c}{c_0}, \quad M = \frac{m}{m_{\max}}, \quad G = \frac{g}{g_0}, \\ &K_C = \frac{k_c}{c_0}, \quad K_G = \frac{k_g}{g_0}, \quad P_e = \frac{vL}{D}, \\ &L_k = \frac{\mu_{\mathrm{m}}L}{v}, \quad M_C = \frac{m_c m_{\max}}{c_0}, \quad M_G = \frac{m_g m_{\max}}{g_0}, \end{aligned} \tag{7}$$

where P_e is the Peclet and L_k the Damkohler number, which describe the ratios of advection rate over dispersion rate and of reaction rate over advection rate, respectively. Here $m_{\max}$ is the maximum microbial mass, which is found by integration of Eq. (3) with respect to time and substitution of boundary conditions:

$$m_{\max} = \frac{g_0}{m_g} + m_0. \tag{8}$$

Substitution of Eq. (7) in Eqs. (1)–(3) yields the dimensionless equations:

$$\frac{\partial C}{\partial T} = \frac{1}{P_e}\frac{\partial^2 C}{\partial X^2} - \frac{\partial C}{\partial X} - M_C\frac{\partial M}{\partial T}, \tag{9}$$

$$\frac{\partial M}{\partial T} = L_k\left(\frac{C}{K_C + C}\right)\left(\frac{G}{K_G + G}\right)M, \tag{10}$$

$$\frac{\partial G}{\partial T} = -M_G\frac{\partial M}{\partial T}. \tag{11}$$

The dimensionless boundary conditions become:

$$-\frac{1}{P_e}\frac{\partial C}{\partial X} + C = 1 \quad \text{for } T > 0 \text{ at } X = 0, \tag{12}$$

$$\frac{\partial C}{\partial X} = 0 \quad \text{for } T > 0 \text{ at } X = 1, \tag{13}$$

$$C = 0, \quad M = \frac{m_0}{m_{\max}}, \quad G = 1 \quad \text{for } X \geqslant 0 \text{ at } T = 0. \tag{14}$$

The coupled system of non-linear partial differential Eqs. (9)–(11) is solved numerically by Keijzer et al. [11]. The numerical results revealed three different time regimes of contaminant consumption. In the third regime, the biodegradation rate is maximal and opposes the dispersive spreading, hence a traveling wave behavior occurs: the fronts of the electron acceptor, the micro-organisms and the organic contaminant approach a constant velocity and fixed shapes while moving through the domain (Fig. 1). Although the contaminant and the microbial mass are immobile, the fronts of these compounds show a traveling wave behavior because during the movement of the electron acceptor, the micro-organisms consume the contaminant and electron acceptor and use them for their growth.

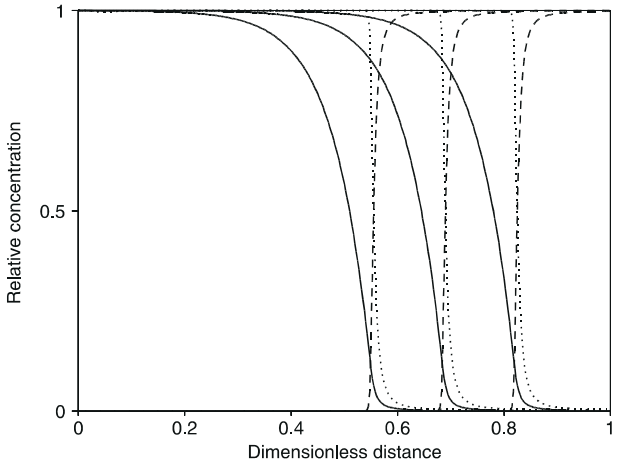

Fig. 1. Relative concentration fronts for electron acceptor (solid line), contaminant (dashed line) and microbial mass (dotted line) at different observation times, obtained by the numerical model.

3. Traveling wave solution

For a traveling wave behavior, analytical solutions may be derived [2,17,22,23]. The traveling wave solution describes the limiting behavior for infinite time and displacement. Keijzer et al. [11] showed that for large L_k, small K_C or small K_G already after a short displacement of time a traveling wave behavior develops. To obtain a traveling wave solution the model equations are transformed to a moving coordinate system, with traveling coordinate η, given by

$$\eta = X - \alpha T, \tag{15}$$

with α the dimensionless traveling wave velocity. An analytical solution for the limiting front velocity follows from mass balance considerations [15,22,23], yielding for the present model [11]

$$\alpha = \left(1 - \frac{M_C}{M_G}\frac{\Delta G}{\Delta C}\right)^{-1}, \tag{16}$$

where $\Delta C = 1$ and $\Delta G = -1$ are the differences between the final and initial conditions for the electron acceptor and contaminant, respectively.

3.1. Traveling wave front shape

Transformation of Eqs. (9)–(11) to the moving coordinate system yields:

$$\frac{1}{P_e}\frac{\mathrm{d}^2 C}{\mathrm{d}\eta^2} = (1-\alpha)\frac{\mathrm{d}C}{\mathrm{d}\eta} - \alpha M_C \frac{\mathrm{d}M}{\mathrm{d}\eta}, \tag{17}$$

$$\alpha\frac{\mathrm{d}M}{\mathrm{d}\eta} = -L_k\left(\frac{C}{K_C + C}\right)\left(\frac{G}{K_G + G}\right)M, \tag{18}$$

$$\frac{\mathrm{d}G}{\mathrm{d}\eta} = -M_G\frac{\mathrm{d}M}{\mathrm{d}\eta}. \tag{19}$$

Assuming that the traveling wave solution is already a good approximation after a relatively short time, we impose the following boundary conditions for the transformed problem [15]:

$$C(\eta) = 1, \quad M(\eta) = 1, \quad G(\eta) = 0, \qquad \text{at } \eta = -\infty, \tag{20}$$

$$C(\eta) = 0, \quad M(\eta) = \frac{m_0}{m_{\max}}, \quad G(\eta) = 1, \quad \text{at } \eta = \infty, \tag{21}$$

where the boundary condition for $C(\eta = -\infty)$ is a reduction of the flux condition (12). It follows that, besides the above conditions, the following conditions also hold

$$\frac{\mathrm{d}C}{\mathrm{d}\eta} = 0, \quad \frac{\mathrm{d}M}{\mathrm{d}\eta} = 0, \quad \frac{\mathrm{d}G}{\mathrm{d}\eta} = 0, \qquad \text{at } \eta = -\infty, \infty. \tag{22}$$

Rather than solving the system (17)–(19), we rewrite the system using the definition

$$w(C) = -\frac{\mathrm{d}C}{\mathrm{d}\eta}. \tag{23}$$

We obtain the following single order differential equation for $w(C)$, see Appendix A

$$\frac{\mathrm{d}w}{\mathrm{d}C} = -P_e(1-\alpha) + P_e(1-\alpha)\left(\frac{L_k M_G}{\alpha w}\right)\left(\frac{C}{K_C + C}\right) \times \left(\frac{G}{K_G + G}\right)\left(1 - \frac{G}{M_G}\right), \tag{24}$$

with $0 \leqslant C \leqslant 1$ and

$$G = -\frac{w}{P_e(1-\alpha)} - C + 1. \tag{25}$$

Furthermore, boundary condition (22) yields

$$w(0) = 0. \tag{26}$$

We integrate Eq. (24) numerically using a fourth-order Runge–Kutta method where the value of $w'(0)$ is found analytically by taking the limit of Eq. (24) for $C \to 0$ $(G \to 1)$ using Eq. (25) and l'Hopital's rule

$$w'(C=0) = -\frac{P_e}{2}(1-\alpha) + \frac{1}{2}\left\{(P_e(1-\alpha))^2 + 4P_e(1-\alpha)\left(\frac{L_k M_G}{\alpha}\right) \times \left(\frac{1}{K_G + 1}\right)\left(1 - \frac{1}{M_G}\right)\left(\frac{1}{K_C}\right)\right\}^{1/2}. \tag{27}$$

With the resulting solution for $w(C)$ we find the front shape $C(\eta)$ by numerical integration of relation (23) from a reference point $\eta = \eta_r$, where we choose arbitrarily $C = 0.5$

$$\eta - \eta_r = -\int_{0.5}^{C} \frac{1}{w(C')}\,\mathrm{d}C' \quad \text{for } 0 \leqslant C \leqslant 1. \tag{28}$$

The front shapes for $G(\eta)$ and $M(\eta)$ are found from Eq. (28), using Eqs. (25) and (A.1), respectively.

3.2. Traveling wave front position

The front shape is given with respect to an arbitrary reference point, see Eq. (28). We determine this point according to mass balance considerations. Assuming a large domain to prevent the electron acceptor from reaching the outlet, the total amount of electron acceptor injected into the domain, C_{inj}, is equal to the amount of electron acceptor still present in the domain, C_{pres}, plus the amount of electron acceptor consumed by the micro-organisms to biodegrade the contaminant, C_{cons}. The mass balance equation for C is

$$C_{\text{inj}} = C_{\text{pres}} + C_{\text{cons}}. \tag{29}$$

In Appendix B, we derive expressions for these quantities, using the dimensionless Eqs. (9)–(11) and boundary conditions (12)–(13) for the original coordinate system.

If we combine Eqs. (B.1), (B.2) and (B.4), Eq. (29) becomes

$$T^* = \int_0^{X^*} C(X, T^*)\,\mathrm{d}X + \frac{M_C}{M_G}\int_0^{X^*}(1 - G(X, T^*))\,\mathrm{d}X \tag{30}$$

with X^* the only unknown. To determine X^*, we use the traveling wave solutions for C and G, denoted by C_{TW} and G_{TW}, respectively, as derived in Section 3.1. We define $\eta^* = X^* - \alpha T^*$, such that $C_{TW}(\eta^*) = \epsilon$, and $\eta_* = -\alpha T^*$. Hence, solving Eq. (30) for X^* is equivalent to finding $\eta^* - \eta^*$ from

$$T^* = \int_{\eta^*}^{\eta^*} C_{TW}(\eta)\,\mathrm{d}\eta + \frac{M_C}{M_G}\int_{\eta^*}^{\eta^*} (1 - G_{TW}(\eta))\,\mathrm{d}\eta. \qquad (31)$$

To achieve this, we use Eq. (28) to write η_r in terms of η^*:

$$\eta^* - \eta_r = -\int_{1/2}^{\epsilon} \frac{1}{w(C')}\,\mathrm{d}C'. \qquad (32)$$

When X^* is found, η_r follows from Eq. (32) by the definition of $\eta^* = X^* - \alpha T^*$ which determines C_{TW} completely.

4. Applicability of the analytical approximation

We derived a traveling wave solution for the biodegradation equations. To show that the traveling wave solution provides a good approximation of the front shape and front position, we carry out a number of numerical simulations and compare the results with the analytical approximations. We apply the numerical method described by Keijzer et al. [11]. An operator-splitting method is applied. The transport part of the equations is solved with a Galerkin finite element method, whereas, the biodegradation reaction part is solved with an implicit Euler method. The two parts are solved using a Picard iteration.

For all simulations the following physical and biochemical parameters are kept constant, the numerical values are chosen in agreement with Schäfer and Kinzelbach [18] and Borden and Bedient [3]. The porosity and velocity are $n = 0.4$ and $v = 0.1$ m/day, respectively, and the length of the domain is $L = 10$ m. The initial available contaminant and microbial mass are $g_0 = 4.5$ mg/l and $m_0 = 0.001$ mg/l, respectively. We consider a relatively small initial contaminant concentration that results in a realistic maximal microbial mass. The imposed mass flux of the electron acceptor at the inlet is vc_0 with $c_0 = 5.0$ mg/l. We choose the discretization and time step such that the grid Peclet and Courant conditions are fulfilled to avoid numerical dispersion and numerical instabilities. This results in $\Delta x = 0.025$ m and $\Delta t = 0.05$ day.

For the reference case (ref), the values of the dimensionless numbers are given in Table 1. The dimensionless numbers are obtained by using the following values for the remaining physical and biochemical parameters, i.e. $\mu_{\mathrm{m}} = 1$ day^{-1}, $m_c = 30$, $m_g = 10$, $k_c = 0.2$ mg/l, $k_g = 2.0$ mg/l and $\alpha_l = 0.5$ m, respectively. The value of α_l may be too large to account for local mixing effects only but we use this value for the purpose of illustration. Variation of one of the remaining physical or biochemical parameters results in a variation of one of the dimensionless numbers. The semi-analytical and numerical results are shown in dimensionless form.

We compare the semi-analytical and numerical results in two alternative ways. First, we compare the obtained fronts for the electron acceptor, contaminant and microbial mass, as is done in Fig. 2 for the reference case. We conclude that the semi-analytical fronts approximate the numerical fronts almost perfectly. Secondly, we can compare the spatial moments of the semi-analytically and numerically obtained fronts for the original coordinate system. Calculating the spatial moments, we only consider the electron acceptor front as the contaminant and microbial mass are functions of C and w, see, respectively Eqs. (25) and (A.1). The first moment of the electron acceptor front describes the average front position [4,11]:

$$M_1 = \int_0^{\infty} X\frac{\partial C}{\partial X}\,\mathrm{d}X. \qquad (33)$$

The second central moment,

$$M_2^c = \int_0^{\infty} (X - M_1)^2\frac{\partial C}{\partial X}\,\mathrm{d}X, \qquad (34)$$

describes the spreading (or variance) of the front. For both the semi-analytical and numerical fronts these moments can be derived numerically with the trapezoidal rule. The first and second central moment for semi-analytical (ana) and numerical (num) fronts are given in Table 1, at specific time T^*. Table 1 shows good agreement between the first and second central moments of the semi-analytical and numerical results for the different cases. We conclude that the traveling wave solution is valid for every value of the different dimensionless numbers, but only applicable to aquifers if the length of the aquifer is long enough [11,15,16]:

5. Parameter sensitivity

In Section 3, we have derived a traveling wave solution that describes the averaged front position and the front shape. Using this solution, we assess the effect of the dimensionless numbers in terms of the averaged front position and the spreading of the front. In view of uncertainties in the physical and biochemical properties in field situations, the dimensionless numbers are varied over a wide range of values.

In Fig. 3, we show the first moment as a function of the dimensionless numbers which are normalized with respect to the reference case (subscript r):

Table 1
Dimensionless numbers and specific time (T^*) that were used to calculate the first and second central moment (M_1 and M_2^c) analytically (ana) and numerically (num). P_e is varied for cases a, L_k for cases b, K_C for cases c, K_G for cases d, M_C for cases e, and M_G for cases f

Case	P_e	L_k	K_C	K_G	M_C	M_G	T^*	$M_{1\text{num}}$	$M^c_{2\text{num}}$	$M_{1\text{ana}}$	$M^c_{2\text{ana}}$
Ref	20	100	0.04	0.4	2.7	1.0022	2.5	0.624	0.0048	0.624	0.0047
*a*1	10	–	–	–	–	–	–	0.577	0.016	0.577	0.016
*a*2	100	–	–	–	–	–	–	0.664	0.00027	0.663	0.00027
*b*1	–	50	–	–	–	–	–	0.623	0.0051	0.622	0.0049
*b*2	–	200	–	–	–	–	–	0.624	0.0047	0.624	0.0044
*c*1	–	–	0.004	–	–	–	–	0.624	0.0046	0.624	0.0045
*c*2	–	–	0.2	–	–	–	–	0.623	0.0054	0.623	0.0056
*d*1	–	–	–	0.04	–	–	–	0.624	0.0047	0.624	0.0047
*d*2	–	–	–	4.0	–	–	–	0.622	0.0061	0.623	0.0061
*e*1	–	–	–	–	1.35	–	2.0	0.798	0.0077	0.800	0.0077
*e*2	–	–	–	–	27.0	–	6.0	0.167	0.0019	0.167	0.0019
*f*1	–	–	–	–	–	1.022	–	0.633	0.0048	0.633	0.0047
*f*2	–	–	–	–	–	1.22	–	0.725	0.0052	0.727	0.0051

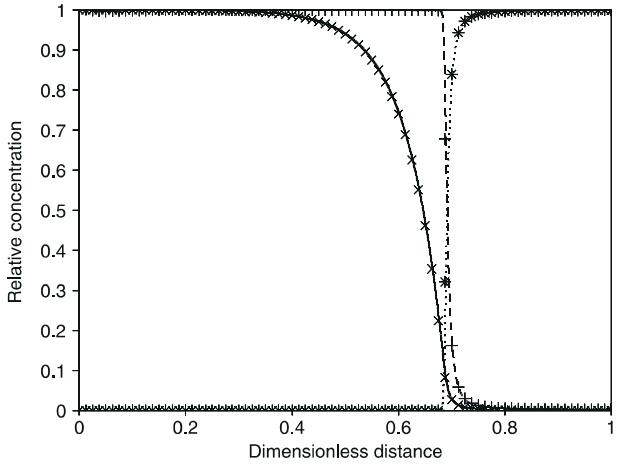

Fig. 2. Relative concentration fronts resulting from analytical and numerical model. Semi-analytical and numerical front for electron acceptor: solid line and ×, contaminant: dotted line and ∗, and microbial mass: dashed line and +.

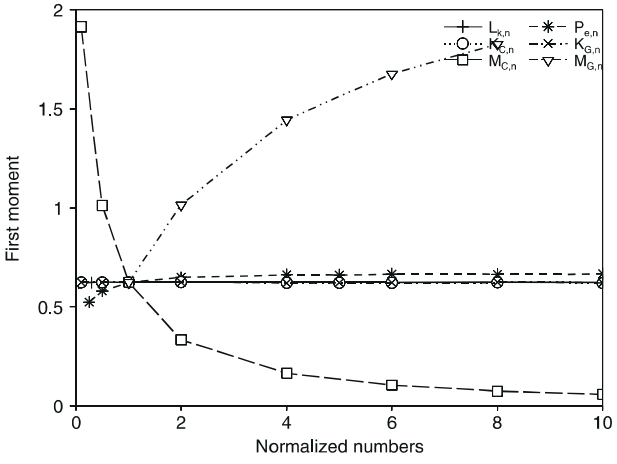

Fig. 3. Dependence of the first moment on the dimensionless numbers, which are normalized with respect to the reference case, for example, $P_{e,n} = P_e/P_{e,r}$.

$$P_{e,n} = \frac{P_e}{P_{e,r}}, \quad L_{k,n} = \frac{L_k}{L_{k,r}},$$
$$K_{C,n} = \frac{K_C}{K_{C,r}}, \quad K_{G,n} = \frac{K_G}{K_{G,r}}, \tag{35}$$
$$M_{C,n} = \frac{M_C}{M_{C,r}}, \quad M_{G,n} = \frac{M_G}{M_{G,r}}.$$

Observe that the Damkohler number, L_k, and the two relative half saturation constants, K_C and K_G, barely affect the first moment, whereas the two relative stoichiometric coeffcients, M_C and M_G, and the Peclet number, P_e, affect the first moment significantly. Because the traveling wave velocity depends on the stoichiometry [11,15,16] decreasing M_C or increasing M_G results in a larger traveling wave velocity. Hence, the front intrudes faster into the domain and the first moment grows faster with time. Although P_e is not part of Eq. (16) it affects the first moment because of the in flux boundary condition (12).

In Fig. 4, we present the second central moment as a function of the normalized dimensionless numbers (35). Increasing P_e, L_k or M_C results in a smaller second central moment, whereas increasing K_C, K_G or M_G results in a larger second central moment. Increasing P_e implies less dispersion, which results in a steeper electron acceptor front and therefore a smaller second central moment. A steeper electron acceptor front also occurs when the microbial growth rate increases. This is indicated by larger L_k values, see Eq. (10). Larger K_C or K_G, on the contrary, induce a smaller microbial growth rate and therefore a less steep electron acceptor front. Furthermore, increasing M_C results in a higher electron

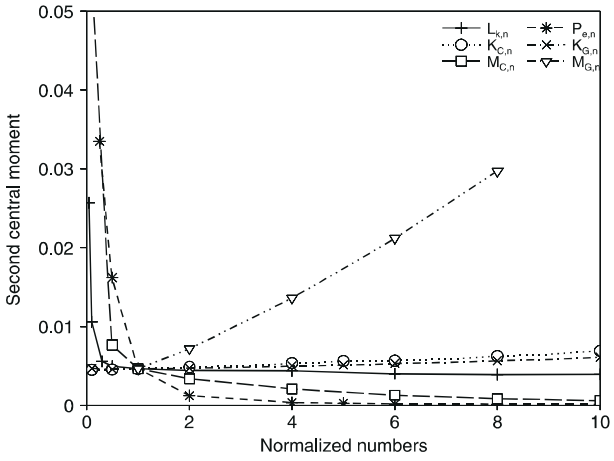

Fig. 4. Dependence of the second central moment on the dimensionless numbers, which are normalized with respect to the reference case, for example, $P_{e,n} = P_e/P_{e,r}$.

acceptor consumption which causes a steeper electron acceptor front, while increasing M_G results in a smaller electron acceptor consumption during the biodegradation of the contaminant, i.e., the electron acceptor front will flatten.

6. Results and discussion

We characterize the performance of in situ bioremediation by the overall contaminant removal rate and the BAZ. We obtain the contaminant removal rate by the same approach as Oya and Valocchi [15,16]. The dimensionless cumulative contaminant removal M_{RG}, for a finite domain, is given by:

$$M_{RG} = n(L^* - \int_0^{L^*} G \, \mathrm{d}X), \tag{36}$$

with n the porosity and L^* the length of the aquifer. The first term on the right-hand side is the total contaminant initially available and the second term is the total contaminant left in the domain. The other term in Eq. (24) of Oya and Valocchi [15] describes the amount of contaminant flowing out of the outlet. This term is omitted because there is no outflow of contaminant at the outlet in our case. The complete term on the right-hand side is defined as the averaged front position of the contaminant [15]. We assume that the traveling wave has developed, the electron acceptor and contaminant front move with the same traveling wave velocity through the domain, thus $\mathrm{d}(L^* - \int_0^{L^*} G \, \mathrm{d}X)/\mathrm{d}T = \alpha$. This leads to the dimensionless contaminant removal rate

$$R_G = \frac{\mathrm{d}M_{rG}}{\mathrm{d}T} = n\alpha = n\frac{1}{1 + \frac{M_C}{M_G}}. \tag{37}$$

The dimensionless contaminant removal rate is proportional to the dimensionless traveling wave velocity and does not depend on L_k, P_e, K_C and K_G, see Eq. (16). This result is also found by Oya and Valocci [15,16] and Borden and Bedient [3]. Using the same approach as above, we obtain the dimensional removal rate

$$r_g = R_G v g_0. \tag{38}$$

which is linearly related to the flow velocity.

We determine the BAZ using the electron acceptor front shape. Although the second central moment describes the overall spreading of the electron acceptor front, it is important whether the entire front or only the part where biodegradation occurs spreads out. Fig. 2, for example, shows that the electron acceptor front spreads mostly out to the left, but that the steep contaminant and microbial mass fronts are situated in a narrow region around the toe of the electron acceptor front. In this situation, the part of the electron acceptor front that is affected by the contaminant and microbial mass is small. If the contaminant front is less steep, a wider region of the electron acceptor front is affected. In this case it is possible that the electron acceptor reaches an extraction well, although still a large amount of contaminant is present in the aquifer.

To determine the influence of the different parameters on the BAZ, we divide the electron acceptor front in two parts. A part where the contaminant and micro-organism fronts are located, see Fig. 2, which is dominated by biodegradation, and a part with virtually zero contaminant and maximal microbial mass, which is dominated by dispersion. We distinguish the two parts of the electron acceptor front on the basis of the function $w(C)$ which denotes the derivative of C with respect to η for each C value, see Eq. (23). According to Eq. (25), we define a critical electron acceptor concentration C_r which separates the two parts:

$$\begin{aligned} &0 < C < C_r, \quad w = -P_e(1-\alpha)[C + G - 1] \\ &\quad \text{(the biodegradation part)} \\ &C_r < C < 1, \quad w = -P_e(1-\alpha)[C - 1] \\ &\quad \text{(the dispersion part)}. \end{aligned} \tag{39}$$

The latter part is linear in C, because $G \approx 0$. For example, Fig. 5 shows $w(C)$ for the reference case, which is non-linear for small C concentrations, the biodegradation-dominated, and virtually linear for larger C concentrations, the dispersion-dominated part, which corresponds to exponential behavior of the left part of the electron acceptor front in Fig. 2.

Using the function $w(C)$, we discuss whether the dimensionless numbers influence the biodegradation or the dispersion-dominated part or both parts of the electron acceptor front. Variation of the Damkohler number L_k (Fig. 6(a)) or one of the relative half saturation constants K_C or K_G (not shown) affects the biodegradation-dominated part of the electron acceptor front and the values of C_r, but not the slope of the linear part in the dispersion-dominated part. This slope is

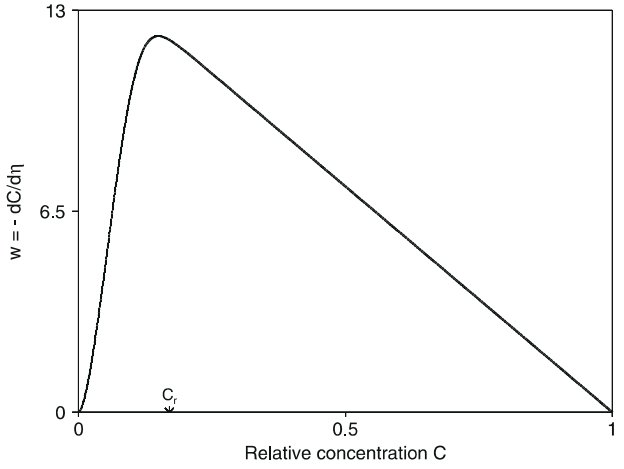

Fig. 5. The function $w(C)$ and the critical electron acceptor concentration C_r for the reference case.

given by the effective Peclet number: $P_{e_{(\mathrm{eff})}} = P_e(1-\alpha)$, see Eq. (39). This behavior is expected because L_k, K_C or K_G are not included in $P_{e_{(\mathrm{eff})}}$ and influence only the microbial growth rate, see Eq. (10). On the other hand, variation of the Peclet number P_e (Fig. 6(b)) or one of the stoichiometric coeffcients M_C or M_G (Fig. 6(c) and (d), respectively) affect also the dispersion-dominated part because $P_{e_{(\mathrm{eff})}}$ is affected too.

Furthermore, we use $w(C)$ to determine the influence of the dimensionless numbers on the BAZ. An increase in C_r leads to a larger biodegradation-dominated part, i.e., a larger BAZ, whereas an increase of $P_{e_{(\mathrm{eff})}}$ results in a steeper electron acceptor front and thus a smaller BAZ. Accordingly, these influences might counteract or intensify each other. We will start with L_k, K_C and K_G and their limiting cases, next P_e and finally M_C and M_G.

Increasing L_k (Fig. 6(a)) or decreasing K_C or K_G (not shown), we obtain a smaller C_r which leads to a larger dispersion-dominated part of the electron acceptor front and, because the slope of the linear part $P_{e_{(\mathrm{eff})}}$ is not affected, to a steeper front shape of the biodegradation-dominated part, see Fig. 7. Hence, the BAZ decreases. This behavior is expected because L_k, K_C and K_G affect the microbial growth, hence the consumption of the electron acceptor.

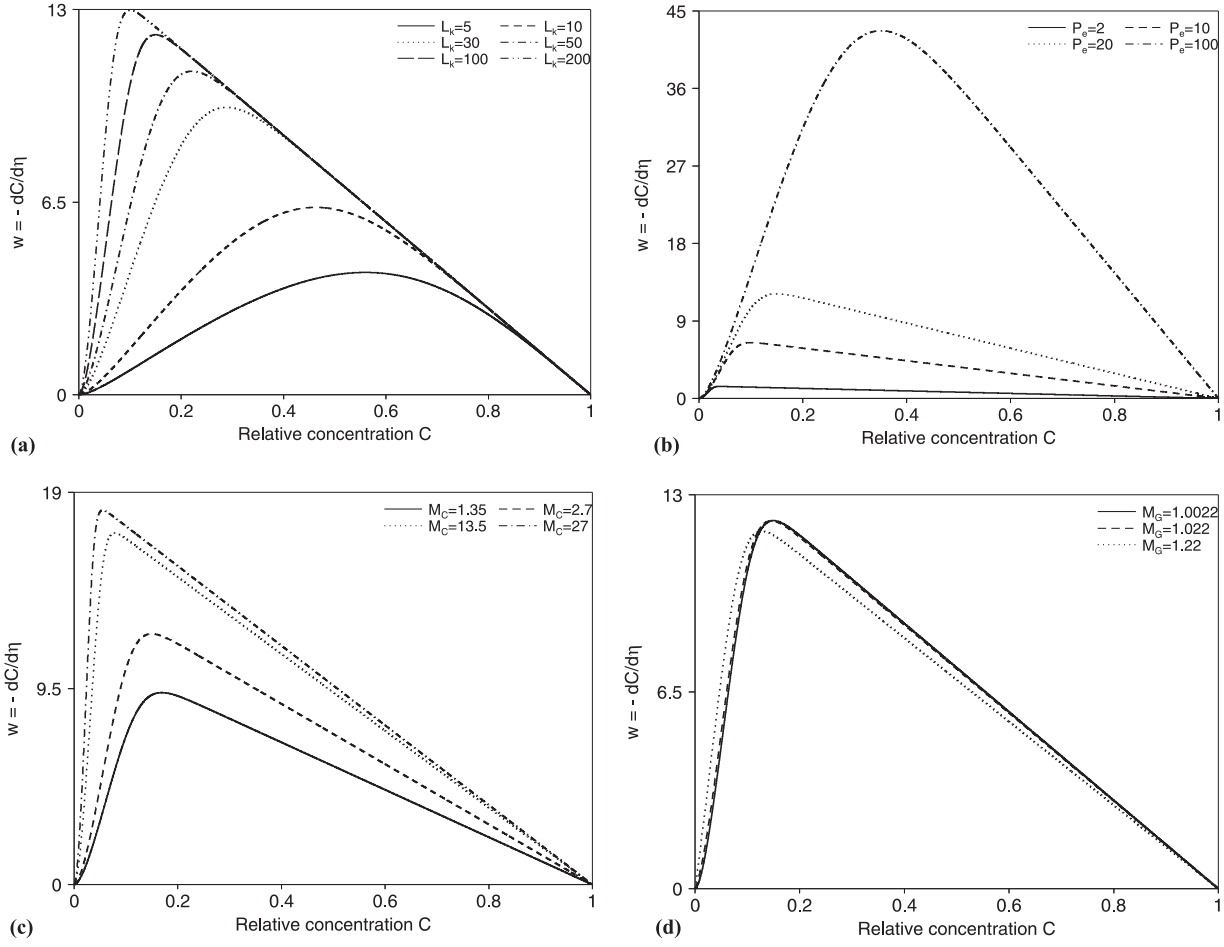

Fig. 6. Influence of parameter variation on $w(C)$ and C_r: (a) Damkohler number L_k, (b) Peclet number P_e, (c) Stoichiometric coefficient M_C and (d) Stoichiometric coefficient M_G.

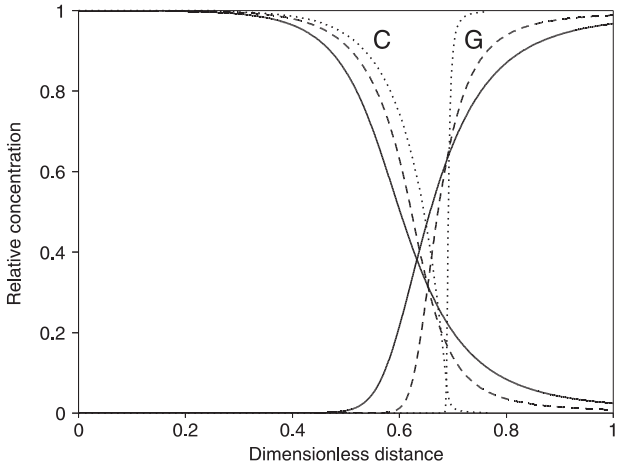

Fig. 7. Relative electron acceptor and contaminant concentration fronts for different Damkohler numbers. (Solid line: $L_k = 5$, dashed line: $L_k = 10$ and dotted line: $L_k = 200$).

Concerning L_k, K_C and K_G, the following limiting cases are of interest: $L_k \to \infty$, indicating fast biodegradation kinetics leading to an equilibrium assumption, $K_C \ll 1$ or $K_G \ll 1$, indicating that electron acceptor or substrate, respectively, are suffciently available [15]. For these limiting situations C_r tends to zero, which implies that the entire electron acceptor front is dominated by dispersion and shows a complete exponential behavior, see Fig. 7. The electron acceptor front shape can be derived analytically from Eq. (39)

$$C(\eta - \eta_r) = 1 - e^{P_e(1-\alpha)(\eta-\eta_r)}, \tag{40}$$

with η_r calculated as explained in Section 3.2. The length of the BAZ is negligible. The contaminant concentration front changes abruptly from initial to zero and is given by a step function. On the other hand, if $L_k \ll 1$, indicating slow biodegradation kinetics, $K_C \gg 1$ or $K_G \gg 1$, indicating that electron acceptor or contaminant, respectively, are limiting factors [15], C_r is equal to one. This implies that the entire electron acceptor front shape is dominated by biodegradation, and the electron acceptor concentration changes only gradually from one to zero, see Fig. 7. Thus a large BAZ is found. Moreover, Keijzer et al. [11] and Oya and Valocchi [15,16] showed that for these specific cases, a long enough aquifer is necessary before the traveling wave can develop.

P_e, M_C and M_G influence both C_r and $P_{e_{(\mathrm{eff})}}$. Fig. 6(b) shows that increasing P_e leads to a larger value of C_r, but also to a larger value of $P_{e_{(\mathrm{eff})}}$. Effectively, w grows with increasing P_e in the biodegradation-dominated part of the electron acceptor front, resulting in a steeper shape of this part of the front. Hence, a smaller BAZ is found.

Fig. 6(c) shows that increasing M_C results in a smaller value of C_r and a larger value of $P_{e_{(\mathrm{eff})}}$, because an increase of M_C results in a smaller traveling wave velocity, see Eq. (16). As a result, the biodegradation-dominated part becomes smaller and the electron acceptor front steepens for increasing M_C. Hence, a smaller BAZ is obtained.

Furthermore, Fig. 6(d) shows that an increase of M_G leads to a smaller value of C_r, but also a smaller value of $P_{e_{(\mathrm{eff})}}$, as an increase of M_G results in a larger traveling wave velocity, see Eq. (16). In the biodegradation-dominated part of the electron acceptor front a larger w is found. Hence, effectively w grows with increasing M_G in the biodegradation-dominated part, resulting in a steeper shape for this part of the front. This implies a decreasing BAZ. We conclude that increasing L_k, M_C, M_G or P_e results in a smaller BAZ, whereas, increasing K_C or K_G results in a larger BAZ. A smaller BAZ implies a more efficient use of electron acceptor, thus increasing L_k, M_C, M_G or P_e or decreasing K_C or K_G results in a better performance of the bioremediation technique.

When we apply the in situ bioremediation technique at a specific contaminated site we may increase the contaminant removal rate, or decrease the BAZ or both, by varying one of the dimensionless numbers. At a specific site, we consider a particular set of contaminant, microbial mass and electron acceptor, for which the following biochemical parameters are fixed: the stoichiometric coefficients (m_c and m_c), the half saturation constants (k_c and k_g) and the specific growth rate (μ_m). Furthermore, the initially available contaminant concentration (g_0), microbial mass (m_0) and the considered contaminated aquifer length (L) are fixed field data. Thus the only parameters with which we can steer the operation are the injection velocity (v) and the injected electron acceptor concentration (c_0). This implies that we can vary L_k, K_C and M_C, whereas the other dimensionless numbers are fixed, see Eq. (7). However, we cannot increase the injection velocity to arbitrary high values because of physical limits and the concentration of injected electron acceptor is limited by the concentration at saturation. This concentration depends on the electron acceptor used, e.g. nitrate has a larger concentration at saturation than oxygen.

Increasing the injection velocity leads to a smaller Damkohler. A smaller L_k implies a larger BAZ, see Fig. 7, because a tailing in the biodegradation dominated part of the electron acceptor front occurs. However, increasing the injection velocity leads also to a higher dimensional contaminant removal rate, see Eq. (38).

Increasing the injected electron acceptor concentration leads to a smaller half saturation constant K_C and a smaller stoichiometric coefficient M_C. The resulting effects counteract because a smaller K_C implies a smaller BAZ, yet, a smaller M_C implies a larger BAZ. Fig. 8 presents the electron acceptor and contaminant fronts for different values of c_0. For larger values of c_0 (e.g., dotted line) a less steep front shape for the biodegradation-dominated part occurs. Hence, the negative effect

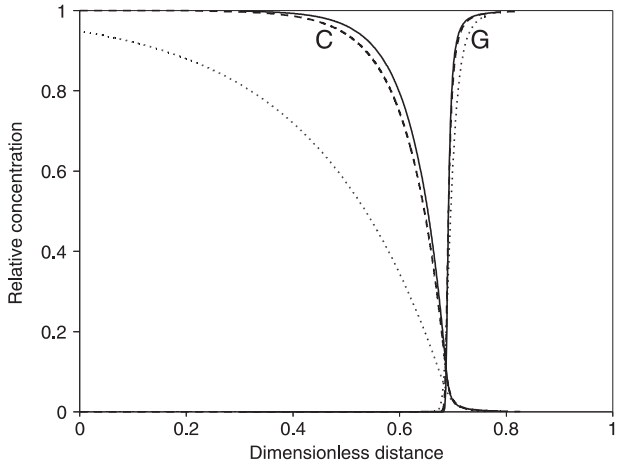

Fig. 8. Relative electron acceptor and contaminant concentration front for different injected electron acceptor concentrations. (Solid line: $C_0 = 2.5$ mg/l, dashed line: $C_0 = 5.0$ mg/l and dotted line: $C_0 = 50.0$ mg/l).

of M_C dominates over the positive effect of K_C, resulting in a larger BAZ. This follows directly from Eq. (A.5), where K_C is included in term $C/(K_C + C)$, and M_C in $M_G L_k/\alpha (= (M_G + M_C)L_k)$. Whatever value we choose for c_0, the first term will always be between zero and one, whereas the other term will always be larger than one. Accordingly, the increase of c_0 influences the term $(M_G + M_C)L_k$ more strongly than the term $C/(K_C + C)$. However, increasing c_0 leads also to a larger dimensionless traveling wave velocity and thus a higher contaminant removal rate, see Eq. (38).

We conclude that increasing the injection velocity or the injected electron acceptor concentration results in a higher contaminant removal rate and a larger BAZ. A higher removal rate and a larger BAZ have counteracting effects on the performance of the bioremediation technique. A higher removal rate causes a faster clean up, whereas, a large BAZ indicates that a large part of the aquifer contains contaminant concentrations between the initial and zero concentration. Therefore, it can take a long time before the contaminant is completely removed by the micro-organisms even though the removal rate expresses differently. If we are interested only in the contaminant removal rate or the BAZ, respectively increasing or decreasing the injection velocity or the injected electron acceptor concentration results in an improvement of the bioremediation technique.

7. Conclusions

We investigated the performance of the in situ bioremediation technique under simplifying assumptions. Because of these simplifying assumptions we can derive an analytical expression for the traveling wave velocity and a semi-analytical solution for the traveling wave front shape of the electron acceptor front. We showed that these solutions perfectly approximate the traveling wave behavior which was found in the numerical results. Furthermore, it is found that this traveling wave solution is valid for all combinations of dimensionless numbers, although in some situations it can take a long time (or traveled distance) before the solution is applicable.

Using the analytical traveling wave velocity and the semi-analytical solution for the front shape, we can determine the contaminant removal rate and the region where biodegradation occurs, the BAZ. These two factors characterize the performance of the bioremediation technique. We showed that the contaminant removal rate is proportional to the traveling wave velocity. Thus a higher traveling wave velocity results in a faster clean up. The BAZ depends on the front shape of the electron acceptor, especially the biodegradation-dominated part of the electron acceptor concentration front. A tailing in the biodegradation-dominant part implies a large BAZ. A large part of the aquifer contains contaminant between initial and zero concentration. Therefore, it can take a long time before the aquifer is cleaned.

Furthermore, we assessed the influence of the different model parameters on the performance of the in situ bioremediation technique. We showed that only the stoichiometric coeffcients, M_C and M_G, influence the traveling wave velocity. Therefore, decreasing M_C or increasing M_G results in a higher contaminant removal rate. All dimensionless numbers influence the biodegradation-dominated part of the electron acceptor front and thus the BAZ. Increasing the Damkohler number, the stoichiometric coeffcients or the Peclet number, or decreasing the relative half saturation constants results in a smaller BAZ and thus in an improvement of the bioremediation technique.

To improve the performance of in situ bioremediation at a specific contaminated site of fixed length, we can only vary the injection velocity or the injected electron acceptor concentration because all other physical and biochemical parameters are fixed. Increasing the injection velocity or the injected electron acceptor concentration results in a higher contaminant removal rate and a larger BAZ, which have counteracting effects on the performance of the bioremediation technique. A higher removal rate implies a faster clean-up, whereas, a larger BAZ indicates the total clean-up of the aquifer can last a long time.

Although the obtained traveling wave solution is based on a simplified biodegradation model, it is useful to predict the effect of physical and biochemical parameters on the performance of the in situ bioremediation technique. Furthermore, it can give rough and quick estimations of the contaminant removal rate and the BAZ by simplifying the conditions at a real site. On can argue that we consider a one-dimensional homoge-

neous aquifer, whereas in practice, an aquifer is neither one-dimensional nor is the permeability of the aquifer constant. In fact, the permeability is space dependent and thus the assumption of homogeneity does not hold. If we envision an aquifer as an ensemble of one-dimensional streamtubes and each streamtube has different physical and biochemical soil properties (e.g. permeability, initially available contaminant) we can mimic a three-dimensional heterogeneous porous media. Using the stochastic-convective approach discussed by other researchers [7,8,10] we may consider field-scale results. This method is only applicable if the transverse dispersion is negligible.

Appendix A. Evaluation of the single first-order differential equation

To rewrite the system (17)–(19), we first integrate Eq. (19) using boundary conditions (20) and (21), which leads to the explicit relation between M and G

$$M = 1 - \frac{G}{M_G}. \tag{A.1}$$

Substitution of $\mathrm{d}M/\mathrm{d}\eta$ following from Eq. (19) in Eqs. (17) and (18) yields

$$\frac{\mathrm{d}^2C}{\mathrm{d}\eta^2} = P_e(1-\alpha)\frac{\mathrm{d}C}{\mathrm{d}\eta} + P_e\alpha\frac{M_C}{M_G}\frac{\mathrm{d}G}{\mathrm{d}\eta}, \tag{A.2}$$

$$\frac{\mathrm{d}G}{\mathrm{d}\eta} = \frac{M_G L_k}{\alpha}\left(\frac{C}{K_C + C}\right)\left(\frac{G}{K_G + G}\right)M. \tag{A.3}$$

Using definition (16) for the dimensionless traveling wave velocity and Eq. (A.1), we obtain

$$\frac{\mathrm{d}^2C}{\mathrm{d}\eta^2} = P_e(1-\alpha)\left[\frac{\mathrm{d}C}{\mathrm{d}\eta} + \frac{\mathrm{d}G}{\mathrm{d}\eta}\right], \tag{A.4}$$

$$\frac{\mathrm{d}G}{\mathrm{d}\eta} = \frac{M_G L_k}{\alpha}\left(\frac{C}{K_C + C}\right)\left(\frac{G}{K_G + G}\right)\left(1 - \frac{G}{M_G}\right). \tag{A.5}$$

Substitution of expression (A.5) for $\mathrm{d}G/\mathrm{d}\eta$ in Eq. (A.4) and using definition (23) for $w(C)$ gives Eq. (24). Furthermore, we derive an explicit relation between G, C and $w(C)$ by integrating Eq. (A.4) from $\eta = -\infty$ to η and using the definition for $w(C)$, which yields Eq. (25).

Appendix B. Evaluation of the mass balance quantities

The total amount of electron acceptor injected into the domain at a specific time, T^*, is equal to the total influx of electron acceptor at the left boundary

$$C_{\mathrm{inj}}(T^*) = \int_0^{T^*} \text{flux}\,|_{X=0}\,\mathrm{d}T = T^*, \tag{B.1}$$

where the flux is given by boundary condition (12). The amount of electron acceptor still present in the domain at T^* is given by

$$C_{\mathrm{pres}}(T^*) = \int_0^{X^*} C(X, T^*)\,\mathrm{d}X, \tag{B.2}$$

where X^* characterizes the length of the domain that still contains the electron acceptor, defined by

$$C(X^*, T^*) = \epsilon \quad \text{and} \quad C(X, T^*) > \epsilon \quad \text{for } X < X^*,$$

with ϵ a small number, say $\epsilon = 0.001$. To derive C_{cons}, we define the consumed contaminant front, $G_{\mathrm{C}}(X, T)$, which equals the initial available contaminant minus the contaminant still present

$$G_{\mathrm{C}}(X, T) = 1 - G(X, T), \tag{B.3}$$

C_{cons} at T^* is related to G_{C} by the stoichiometric coeffcients, M_C and M_G. M_C describes the amount of electron acceptor necessary to produce a certain amount of microbial mass, and M_G describes the amount of contaminant necessary to produce the same amount of microbial mass, therefore, C_{cons} is given by

$$\begin{aligned} C_{\mathrm{cons}}(T^*) &= \frac{M_C}{M_G}\int_0^{X^*} G_{\mathrm{C}}(X, T^*)\,\mathrm{d}x \\ &= \frac{M_C}{M_G}\int_0^{X^*} (1 - G(X, T^*))\,\mathrm{d}X, \end{aligned} \tag{B.4}$$

where X^* satisfies additionally

$$1 - G(X^*, T^*) \leqslant \epsilon \quad \text{and} \quad 1 - G(X, T^*) > \epsilon \quad \text{for } X < X^*.$$

References

[1] Baveye P, Valocchi AJ. An evaluation of mathematical models of the transport of biologically reacting solutes in saturated soils and aquifers. Water Resources Research 1989;25:1413–21.

[2] Bolt GH. In: Bolt GH, editor. Soil Chemistry B. Physico-Chemical Models. New York:Elsevier, 1982, p. 285.

[3] Borden RC, Bedient PB. Transport of dissolved hydrocarbons influenced by oxygen-limited biodegradation 1. Theoretical development. Water Resources Research 1986;22:1973–82.

[4] Bosma WJP, van der Zee SEATM. Transport of reactive solute in a one-dimensional chemically heterogeneous porous medium. Water Resources Research 1993;29:117–31.

[5] Chen Y, Abriola LM, Alvarez PJJ, Anid PJ, Vogel TM. Modeling transport and biodegradation of benzene and toluene in sandy aquifer material: Comparisons with experimental measurements. Water Resources Research 1992;28:1833–47.

[6] Corapcioglu MY, Kim S. Modeling facilitated contaminant transport by mobile bacteria. Water Resources Research 1995;31:2639–47.

[7] Cvetkovic VD, Shapiro AM, Mass arrival of sorptive solute in heterogeneous porous media. Water Resources Research 1990;26:2057–67.

[8] Destouni G, Cvetkovic VD. Field scale mass arrival of sorptive solute into the groundwater. Water Resources Research 1991;27:1315–25.

[9] Ghiorse WC, Balkwill DL. Enumeration and morphological characterization of bacteria indigenous to subsurface environments. Dev Ind Microbiol 1983;24:213–24.

[10] Ginn TR, Simmons CS, Wood BD. Stochastic-convective transport with non-linear reaction: Biodegradation with microbial growth. Water Resources Research 1995;31:2689–700.

[11] Keijzer H, van der Zee SEATM, Leijnse A. Characteristic regimes for in situ bioremediation of aquifers by injecting water containing an electron acceptor. Computational Geosciences 1998;2:1–22.
[12] Kindred JS, Celia MA. Contaminant transport and biodegradation 2. Conceptual model and test simulations. Water Resources Research 1989;25:1149–59.
[13] Kinzelbach W, Schäfer W, Herzer J. Numerical modeling of natural and enhanced denitrification processes in aquifers. Water Resources Research 1991;27:1123–35.
[14] Monod J. The growth of bacterial cultures. Annual Review of Microbial. 1949;3:371–94.
[15] Oya S, Valocchi AJ. Characterization of traveling waves and analytical estimation of pollutant removal in one-dimensional subsurface bioremediation modeling. Water Resources Research 1997;33:1117–27.
[16] Oya S, Valocchi AJ. Analytical approximation of biodegradation rate for in situ bioremediation of groundwater under ideal radial flow conditions. Journal of Contaminant Hydrology 1998;31:65–83.
[17] Reiniger P, Bolt GH. Theory of chromatography and its application to cation exchange in soils. Netherland Journal of Agricultural Science 1972;20:301–13.
[18] Schäfer W, Kinzelbach W. In: Hinchee RE, Olfenbuttel RF, editors. In Situ Bioreclamation, Numerical Investigation into the Effect of Aquifer Heterogeneity on In Situ Bioremediation. London: Butterworth–Heinemann, 1991, p. 196.
[19] Semprini L, McCarty PL. Comparison between model simulations and field results for in situ biorestoration of chlorinated aliphatics: Part 1. Biostimulation of methanotrophic bacteria. Gound Water 1991;29:365–74.
[20] Stumm W, Morgan JJ. In: Aquatic Chemistry. New York:Wiley, 1981, p. 780.
[21] Sturman PJ, Stewart PS, Cunnungham AB, Bouwer EJ, Wolfram JH. Engineering scale-up of in situ bioremediation process: a review. Journal of Contaminant Hydrology 1995;19:171–203.
[22] Van der Zee SEATM, Analytical traveling wave solutions for transport with non-linear and non-equilibrium adsorption. Water Resources Research 1990;26:2563–78. (Correction, Water Resources Research 1991;27:983).
[23] Van Duijn CJ, Knabner P, van der Zee SEATM, Travelling waves during the transport of reactive solute in porous media: combination of Langmuir and Freundlich isotherms. Advances in Water Resources 1993;16:97–105.
[24] Xin J, Zhang D. Stochastic analysis of biodegradation fronts in one-dimensional heterogeneous porous media. Advances in Water Resources 1998;22:103–16.
[25] Zysset A, Stauffer F, Dracos T. Modeling of reactive groundwater transport governed by biodegradation. Water Resources Research 1994;30:2423–34.